Experimental Investigation of Cycle-by-Cycle Variations in CAI/HCCI Combustion of Gasoline and Methanol Fuelled Engine

Article *in* SAE Technical Papers · April 2009

DOI: 10.4271/2009-01-1345

Avinash Kumar Agarwal
Indian Institute of Technology Kanpur

2009-01-1345

Experimental Investigation of cycle-by-cycle variations in CAI/HCCI Combustion of Gasoline and Methanol fuelled Engine

Rakesh Kumar Maurya, Avinash Kumar Agarwal
Engine Research laboratory,
Department of Mechanical Engineering
Indian Institute of Technology Kanpur
Kanpur – 208016, India
Corresponding author's email: akag@iitk.ac.in

ABSTRACT

The development of vehicles continues to be determined by increasingly stringent emissions standards including CO2 emissions and fuel consumption. To fulfill the simultaneous emission requirements for near zero pollutant and low CO2 levels, which are the challenges of future powertrains, many research studies are currently being carried out world over on new engine combustion process, such as Controlled Auto Ignition (CAI) for gasoline engines and Homogeneous Charge Compression Ignition (HCCI) for diesel engines. In HCCI combustion engine, ignition timing and combustion rates are dominated by physical and chemical properties of fuel/air/residual gas mixtures, boundary conditions including ambient temperature, pressure, and humidity and engine operating conditions such as load, speed etc. Because of large variability of these factors, wide cycle-to-cycle variations are observed in HCCI combustion engines, similarly small variations in ignition timing and combustion rates result in wide variation in engine performance and emissions. Also, cycle-to-cycle combustion variations result in objectionable engine noise and vibrations. As a result of wide cycle-to-cycle variations, HCCI combustion can be achieved in an engine for narrow range of lean and rich operating limits. This motivates the researchers to systematically investigate mechanism and control of cycle-to-cycle variations on HCCI engines.

In this paper, the combustion stabilities and cycle-to-cycle variations of a HCCI combustion engine fuelled with gasoline and methanol were investigated on a modified two-cylinder, four-stroke engine. In this investigation, port fuel injection technique is used for preparing homogeneous charge. The experiment is conducted with variable intake air temperature at different air-fuel ratios at constant engine speed. In-cylinder pressure of 100 combustion cycles for each test condition was recorded. Consequently, cycle-to-cycle variations of the main combustion parameters and performance parameters were analyzed and evaluated. To evaluate the cycle-to-cycle variations of HCCI combustion parameters at various test conditions, coefficient of variation (COV) of each parameter was used. The results show that critical parameters, which can be used to define HCCI operating range, are maximum rate of pressure rise, and COV of indicated mean effective pressure (IMEP).

INTRODUCTION

Ever since CO2 is identified as a greenhouse gas contributing to global warming, diesel engines are emerging strongly as an alternative to gasoline engines due to lower fuel consumption and lower CO2 emission potential. Carbon monoxide (CO) emission are negligible in CI engines due to its lean operation and emissions of unburnt hydrocarbons (HC) can be easily handled using oxidation catalysts however the emissions of oxides of nitrogen (NOx) and particulate matter (PM) remains a major concern from diesel engines.

For Diesel engines, exhaust gas after-treatment and implementation issues usually carry high cost premiums. An alternative is to use a cleaner combustion mode in

The Engineering Meetings Board has approved this paper for publication. It has successfully completed SAE's peer review process under the supervision of the session organizer. This process requires a minimum of three (3) reviews by industry experts.

ISSN 0148-7191

the first place thereby eliminating the need for exhaust gas after-treatment. Therefore, the Highly Premixed Combustion mode (HPC), including Homogeneous Charge Compression Ignition (HCCI) has become of great interest in recent years. HCCI was identified as a distinct combustion phenomenon about 30 years ago [1-2]. HCCI combustion principle consists of preparing air/fuel mixture, highly diluted by burned gas, in achieving its simultaneous ignition at several points, thus precisely controlling the combustion for the best performance in terms of efficiency and emissions. HCCI or HPC combustion takes place in more or less homogeneous manner throughout the bulk of the mixture, and thermal NOx formation and soot production are reported to be significantly lesser than typical conventional diffusion flame in a compression ignition combustion mode [3].

The HCCI combustion process has been studied with reasonable success in two stroke [1, 4] and four stroke engines [5-11], with liquid [1-9] and gaseous fuels [10-12]. The HCCI family can be classified according to the fuel introduction strategy employed [13]. This classification include external fuel injection [14], port injection [5-6], early in-cylinder injection [8, 15-16], late in-cylinder injection [17], and dual fuel introduction (both in-cylinder and port injection) [13].

The main problem with the HCCI is that the ignition is completely controlled by chemical kinetics and is therefore affected by fuel composition, equivalence ratio, and thermodynamic state of air-fuel mixture [18]. There is no external control such as fuel injection or spark timing that are used in CI or SI engines. Achieving the required level of control during transient engine operation is even more challenging since charge temperature has to be correctly matched to the operating condition during rapid transients with a high repeatability since the speed and load is changing. The ignition timing and combustion rates are dominated by physical and chemical properties of fuel/ air/ residual gas mixtures, boundary conditions including ambient temperature, pressure, humidity and engine operating conditions such as load, and speed. Because of these variables, wide cycle-to-cycle variations are observed in HCCI combustion engines [19]. Even small changes in ignition timing and combustion rate bring large variation in engine performance and emissions [19]. As a result, wide cycle-to-cycle variations restrict the lean and rich operating limits of HCCI combustion engine. Understanding cycle-to-cycle variations in combustion process are essential because they play important role in combustion stability and operating limit decision for the HCCI engine operating range. Many researchers reported coefficient of variation of IMEP (COVIMEP) and maximum rate of pressure rise as HCCI operating region criteria [20-21].

Cycle-to-cycle combustion variability is a prominent characteristic of spark ignition engine operation also [22]. Changes in the combustion environment from one cycle to the next may result in significant variation in combustion events. These cycle-to-cycle variations in the combustion will be reflected in fluctuation in cylinder pressure, which in turn, will be manifested as variation in power output. Depending on the severity of the combustion variability, resulting power variations may be objectionable to the driver, or they may only be detectable through precise measurement of the engine performance. Cycle-to-cycle combustion variations present a challenge to the engine designers for several reasons. Since satisfying the customer is the primary goal of any automotive manufacturer, consumer's perception of the engine "smoothness" is an important concern. Cyclic variations results in non-uniform power delivery, uneven acceleration or a shaky idle condition, which can be felt by driver and as a result, vehicle drivability suffers. Studies have also showed that cycle-to-cycle pressure variations in the in-cylinder pressure also contribute to engine noise [23]. Spark ignition engine studies suggest that complete elimination of cycle-to-cycle combustion variations would result in up to 10% improvement in power output for the same fuel consumptions [24].

Mechanism and control of cycle-to-cycle variation in SI engines are systematically investigated by several researchers [25-28]. However very limited research work is reported on cycle-to-cycle variations and combustion stability of HCCI combustion. Xingcai et al. investigated the combustion stabilities and cycle-to-cycle variations of HCCI combustion using n-heptane, primary reference fuels 20 (PRF20), PRF40, PRF50 and PRF60 [19]. Persson performed preliminary study on the cylinder-to-cylinder and cycle–to-cycle variations of CAI (controlled auto ignition) combustion with trapped residual gas [29]. Koopmans et al. investigated the cycle-to-cycle variations in a camless gasoline fuelled compression ignition engine [30]. Shi et al. investigated combustion stability of diesel fuelled HCCI and effect of engine load, speed and valve overlap [31]. To gain an improved understanding of HCCI combustion, a systematic study of cycle-to-cycle variation of HCCI combustion is essential. The objective of this study is to investigate the effect of intake air temperature and air-fuel ratio on cycle-to-cycle variations in a methanol and gasoline fueled port injection HCCI engine operating at constant engine speed (1500 rpm).

EXPERIMENTAL SETUP

A two cylinder, four-stroke, air cooled, naturally aspirated, direct injection diesel engine was modified for the experiment. The engine specifications of unmodified engine are given in table 1. One of the two cylinders of the engine is modified to operate in HCCI mode, while the other cylinder is operated like an ordinary diesel engine, which provides motive power for operating the first cylinder. A schematic diagram of the experimental setup is shown in Figure 1.

Table 1: Specification of test engine

Engine Characteristics	Specification
Make/ Model	Indec/ PH2
Injection Type	Direct Injection
Number of Cylinders	Two
Bore / Stroke	87.3 / 110 mm
Power per Cylinder	4.85 kW @ 1500 rpm
Compression Ratio	16.5
Displacement	1318 cc
Fuel Injection Timing	24^0 before TDC
Fuel Injection Pressure	210 kg/cm^2 @1500 rpm
Combustion Chamber	Bowl-shaped

Test fuels used for this investigation are methanol and gasoline. A fuel premixing system was installed in the intake manifold. This system consists of electronic gasoline port injector and an injection timing and injection duration controlling electronic circuit. Controlling circuit developed for this purpose is used to control the pulse width, which in turn triggers the fuel injector. Fresh air entering the engine is heated by an air pre-heater positioned upstream of the intake manifold. The intake air heater is operated by a closed loop controller, which maintains constant intake air temperature as set by user by feed-back control. A thermocouple in conjunction with a digital temperature indicator was used in measuring the intake and exhaust gas temperature. An orifice meter was used to measure air consumption of the engine with the help of a U-tube manometer. A surge tank fixed on the inlet side of the engine maintains a constant air flow through orifice meter.

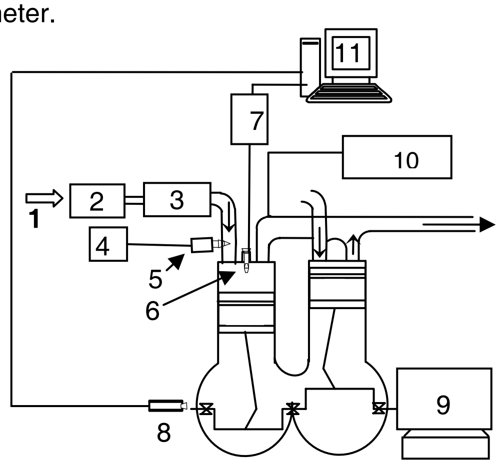

1: Intake Air, 2: Air Box, 3: Heater, 4: Injection Timing Circuit, 5: Electronic fuel Injector, 6: Piezo-electric Pressure Transducer, 7: Charge Amplifier, 8: Shaft Encoder, 9: Dynamometer, 10: Emission Analyzer, 11: Combustion analyzer

Figure 1: Schematic diagram of experimental setup

The in-cylinder pressure was measured using a water-cooled piezo-electric pressure transducer (Make: Kistler, Switzerland; Model: 6061B; Range 0-250 bar), which is mounted flush in the cylinder head. The pressure transducer minimizes thermal shock error by using a double walled diaphragm and integral water cooling system. A crank angle encoder was used to sense the position of top dead center (TDC). To measure the CAD, a precision shaft encoder (Make: Encoders India, Model: ENC58/6-720ABZ/5-24V) is coupled with the crank-shaft using a helical coupling. The cylinder pressure history data acquisition and combustion and cycle-to-cycle variation analysis is done using a computer program based on LabVIEW, developed at Engine Research Laboratory, IIT Kanpur for this purpose.

Experiments were conducted at constant engine speed of 1500 rpm and varying intake air temperatures ranging from 110-160^{0}C at different air-fuel ratios for each intake air temperature.

DEFINITIONS OF COMBUSTION PARAMETERS

To study the cycle-to-cycle variations of typical HCCI combustion and performance characteristics at different engine test conditions, following parameters are analyzed

- Relative Air Fuel ratio (λ): ratio of the actual air/fuel ratio to the stoichiometric air/ fuel ratio.
- P_{max}: Maximum gas pressure in the cylinder
- $\theta_{P\max}$: Crank Angle corresponding to P_{max}
- $\left(dP/d\theta\right)_{\max}$: Maximum rate of pressure rise
- $\theta_{(dP/d\theta)_{\max}}$: Crank angle corresponding to maximum rate of pressure rise
- Rate of heat release (ROHR): Calculated from the acquired data using the zero dimensional heat release model [32]. Consequently, the main combustion parameters were extracted from the heat release and in-cylinder pressure curves. ROHR was calculated as

$$\frac{dQ(\theta)}{d\theta} = \left(\frac{1}{\gamma-1}\right)V(\theta)\frac{dP(\theta)}{d\theta} + \left(\frac{\gamma}{\gamma-1}\right)P(\theta)\frac{dV(\theta)}{d\theta}$$

The following assumptions were made in this calculation:

- o Cylinder charge was considered to behave as an ideal gas.
- o Distribution of thermodynamic properties inside the combustion chamber was considered to be uniform.
- o Dissociation of combustion products was neglected.
- o No variation of cylinder mass due to blow-by was considered.
- o Heat transfer from the cylinder is neglected in this model.

- $ROHR_{max}$: Maximum rate of heat release in a cycle.
- $\theta_{ROHR_{\max}}$: Crank angle corresponding to $ROHR_{max}$
- Indicated Mean Effective Pressure (IMEP): is the ratio of work per cycle by volumetric displacement of engine.
- Mean gas temperature: Calculated by assuming uniform temperature within the engine cylinder using ideal gas law [32]. The results are valid between IVC (intake valve closing) and EVO (exhaust valve opening).

$$T(\theta) = \frac{P(\theta)V(\theta)n(\theta)}{P_{IVC}V_{IVC}n_{IVC}}T_{IVC}$$

In this calculation, molar ratio is assumed to be unity.

RESULTS AND DISCUSSION

In this section the experimental results at different engine operating conditions are presented. To evaluate the cycle-to-cycle variations of HCCI combustion at various test conditions, coefficient of variation (COV) of combustion parameters was found. COV of any parameter was calculated using following equations.

$$COV(x) = \frac{\sigma}{\bar{x}} \times 100\%$$

Where $\bar{x} = \sum_{i=1}^{n} x_i / n$ and standard deviation (σ)

$$\sigma = \sqrt{\sum_{i=1}^{n} \left(x_i - \bar{x}\right)^2 / (n-1)} \quad [19]$$

Engine operating parameters like intake air temperature, air-fuel ratio, engine speed, properties of test fuel etc. play important role in combustion stability and cycle-to-cycle variation in HCCI combustion. In the following section, cycle-to-cycle variation of P_{max}, $\theta_{P\max}$, $\left(dP/d\theta\right)_{\max}$, $\theta_{(dP/d\theta)_{\max}}$, $ROHR_{max}$, $\theta_{ROHR_{\max}}$ and maximum mean gas temperature under different engine operating conditions are analyzed and discussed.

CYCLE-TO-CYCLE VARIATION ANALYSIS

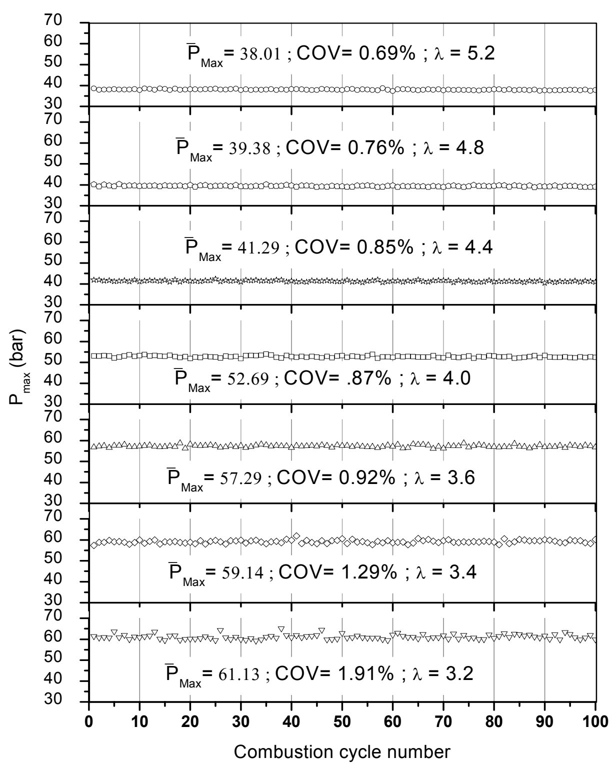

Figure 2: Cycle-to-cycle variation of P_{max} at intake air temperature 120^{0}C for methanol

The in-cylinder pressure was measured using high-precision, water cooled piezo-electric pressure transducer. The cylinder pressure was recorded for consecutive 100 cycles, with a resolution of 0.5 crank angle degrees. Figures 2-3 show the cycle-to-cycle variations of the maximum gas pressure (P_{max}) in the combustion chamber for 100 cycles for each test point using methanol and gasoline as fuel. For every plot, highest average maximum pressure corresponds to the operating conditions with richest air-fuel mixture and lowest average maximum pressure corresponds to leanest air-fuel mixture for methanol and gasoline. At 120^{0}C, the engine could be operated in HCCI mode with relative air-fuel ratio (λ) ranging to 3.2-5.2 for methanol and 2.6-3.8 for gasoline.

It can also be clearly observed from the figures 2-3 that the richer air-fuel mixtures lead to relatively higher COV and as mixture becomes leaner, the COV decreases. This trend is observed for both, gasoline and methanol. The maximum gas pressure in 100 cycles for methanol and gasoline shows similar cycle-to-cycle variations at intake air temperature of 120^{0}C. For all engine test conditions P_{max} deviated in narrow range for both fuels. It can be observed from these figures that for all test points, the variation in maximum in-cylinder pressure is rather small (COV < 2%).

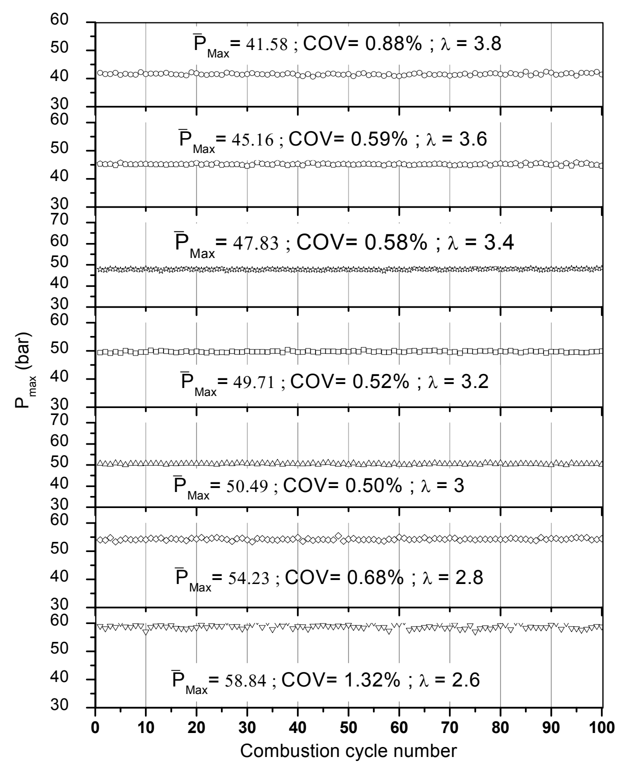

Figure 3: Cycle-to-cycle variation of P_{max} at intake air temperature 120$^°$C for gasoline

Apart from cycle-to-cycle variations of maximum gas pressure, it is also important to note the variations in crank angle position, at which maximum pressure is obtained. Since in HCCI combustion, there is no direct control of start of combustion, ignition is completely controlled by chemical kinetics and is therefore affected by fuel composition, equivalence ratio, and thermodynamic state of the fuel-air mixture. So, it has possibility of cycle-to-cycle variations in positions where combustion starts, which in turn affect the position of maximum gas pressure in the cycle. Figures 4-5 show the frequency distribution of crank angle corresponding to P_{max}. It is essential to have the CAD corresponding to maximum gas cylinder pressure $\theta_{P\max}$ near top dead center (TDC) of piston for optimum engine efficiency. The power generation in the cycle is hampered in both cases either because of too much delay or advance in $\theta_{P\max}$. The study of variation of this parameter is important to relate variation in power generated in the cycle. It can be seen from these figures that crank angle distribution is concentrated more near average $\theta_{P\max}$ and scattered around average value for the richer mixtures.

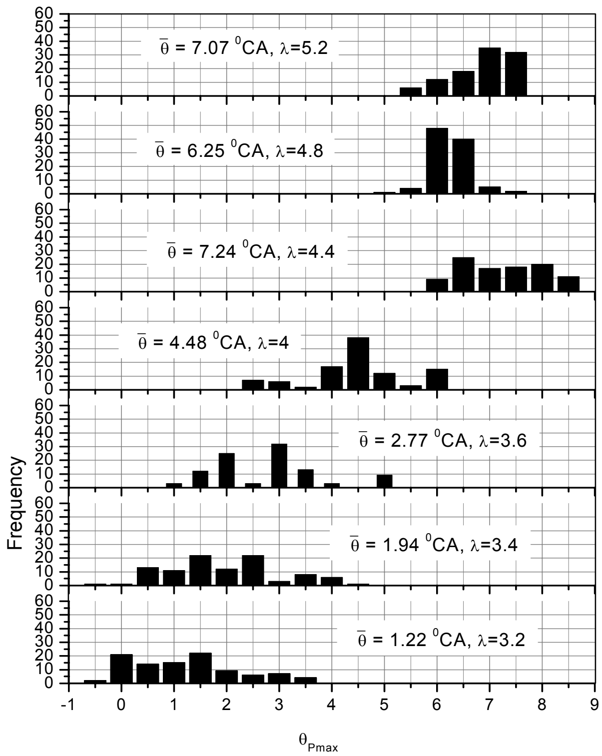

Figure 4: Frequency distribution of crank angle corresponding to P_{max} at intake air temperature 120^0C for methanol

It can be observed from the figures that as mixture become leaner, the average value of the $\theta_{P\max}$ increase after TDC for both fuels. Richer mixture ignites earlier compared to leaner mixture at same intake air temperature since these operating conditions have higher load and combustion temperatures and thus higher residual mixture temperature, which results is higher fuel-air-residual gas temperature leading to earlier ignition, closer to TDC. It can also be observed from the figures 4-5 that, for both fuels (methanol and gasoline), repeatability of CAD P_{max} increases as mixture becomes leaner for constant intake air temperature. It is observed that for all test conditions for methanol, the maximum repeatability of $\theta_{P\max}$ is less than 50 percent, however gasoline has maximum repeatability up to 70 percent at intake air temperature of 120^0C.

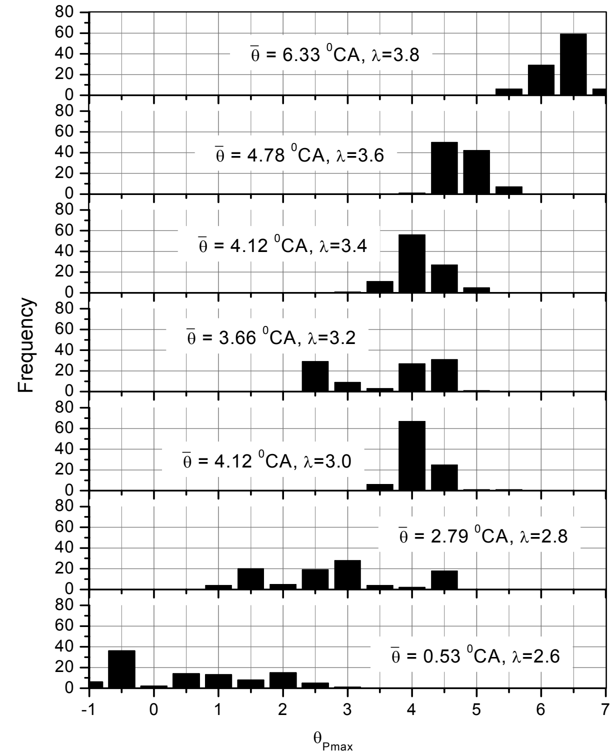

Figure 5: Frequency distribution of crank angle corresponding to P_{max} at intake air temperature 120^0C for gasoline

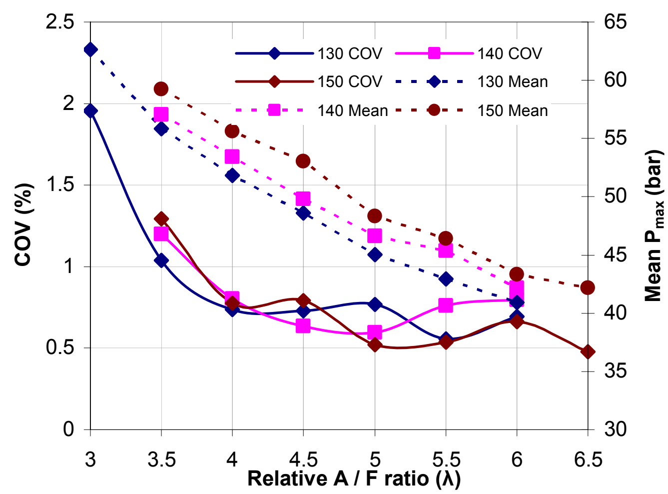

Figure 6: Cycle-to-cycle variation of P_{max} for methanol at different intake air temperatures

Figures 6-7 show the cycle-to-cycle variations of P_{max} using methanol and gasoline at different intake air temperatures and air-fuel mixtures. Figures show Coefficient of Variation (COV) and mean maximum gas pressure of 100 cycles at each test conditions for both fuels. Mean values are connected by dotted lines and COV are connected by solid lines. Similar trends are observed at all intake air temperatures for both fuels in terms of COV and average maximum gas pressure. Average P_{max} decreases as mixture becomes leaner at any constant intake air temperature.

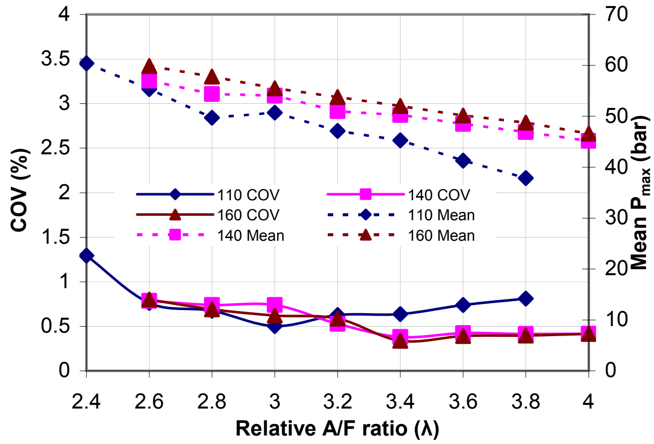

Figure 7: Cycle-to-C=cycle variation of P_{max} for gasoline at different intake air temperatures

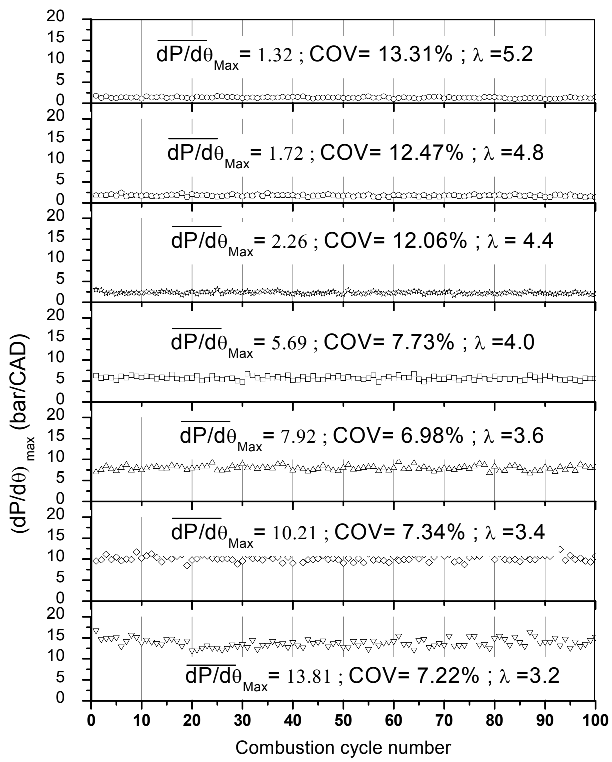

Figure 8: Cycle-to-cycle variation of $(dP/d\theta)_{max}$ at intake air temperature 120^{0}C for methanol

It is observed from figures 6-7 that average value of maximum gas pressure increases with increasing intake air temperature at constant relative air fuel ratio (λ) and decreases as values of λ increases. It can also be observed from these figures that at all intake air temperatures, COV of P_{max} is less than 2 percent for both methanol and gasoline. It can also be noticed that in HCCI combustion, cycle-to-cycle variation in maximum gas pressure is small (COV<2%) for the experimental conditions. This observation is justified because of the auto-ignition process, since there is no flame propagation as observed in a SI combustion engine hence maximum gas pressure deviate in a very small range.

Figures 8-11 show cycle-to-cycle variations of maximum rate of pressure rise in the cycle and statistical analysis of crank angle degree corresponding to maximum rate of pressure rise for 100 consecutive combustion cycles at all engine test points at intake air temperature of 120^{0}C.

Rate of pressure rise is related to combustion noise generated in the engine. When the fuelling rates are increased (i.e. lower λ), the HCCI combustion rates increase and intensify, and gradually cause unacceptable noise and potentially cause engine damage, which may eventually lead to unacceptably high level of NOx emissions. Therefore knocking combustion is often used to define the upper limit of HCCI.

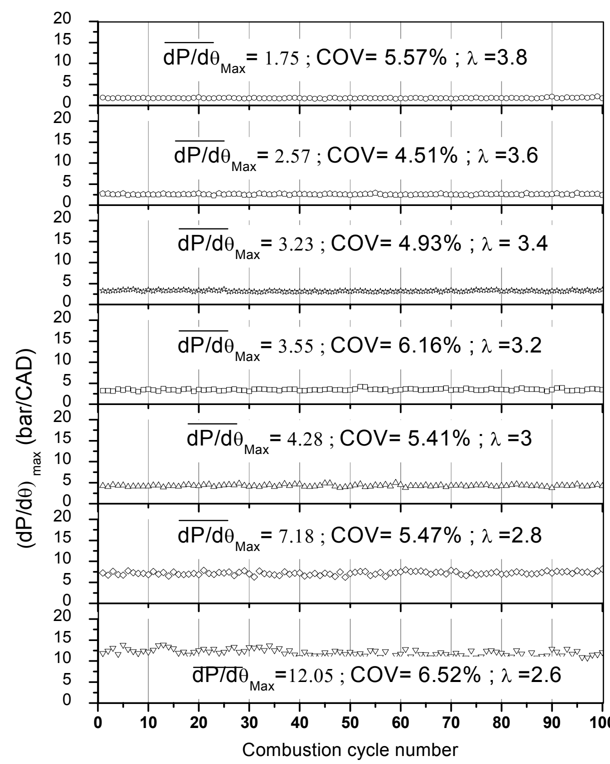

Figure 9: Cycle-to-cycle variation of $(dP/d\theta)_{max}$ at intake air temperature 120^{0}C for gasoline.

It can be seen from figures 8-9 that average rate of pressure rise is very high for richer fuel-air mixtures and is rather low for leaner fuel-air mixtures. Rate of combustion is critical parameter to control in HCCI combustion. For richer mixture, the rate of combustion is very high for both fuels. Engine becomes very noisy when running on richer mixture. This is explained by high average rate of pressure rise. The variation in the value of COV of $(dP/d\theta)_{max}$ is more than 10 percent for some engine operating conditions at intake air temperature of 120^{0}C. The COV of maximum rate of pressure rise is higher as compared to maximum gas pressure. Cycle-to-cycle variation of maximum rate of pressure is lower for gasoline as compared to methanol at intake air temperature of 120^{0}C. For richer engine operating condition, the average rate of pressure rise is very high compared to value of COV. The value COV can be lower for higher rate of pressure rise, which generate enormous amount of combustion noise. Hence it can be concluded that for determination of upper boundary of HCCI, average value of $(dP/d\theta)_{max}$ is a better parameter compared to COV of $(dP/d\theta)_{max}$.

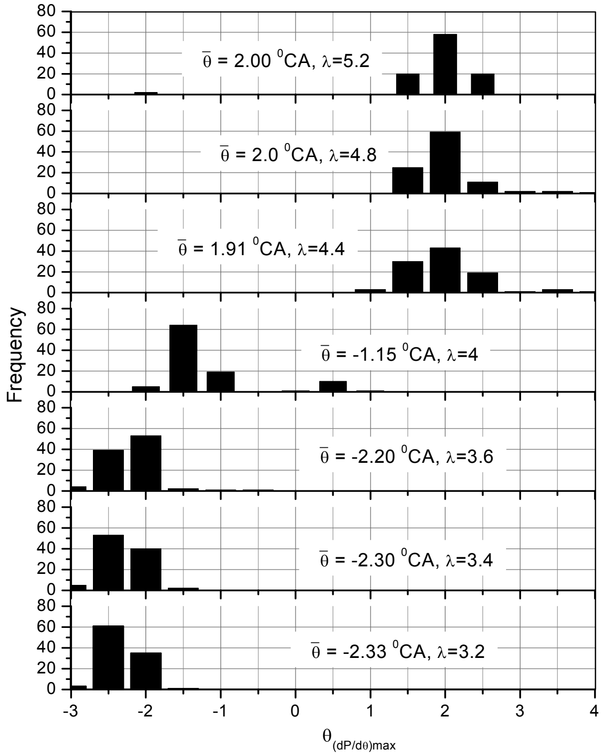

Figure 10: Frequency distribution of crank angle corresponding to $(dP/d\theta)_{max}$ at intake air temperature 120^{0}C for methanol

It can be seen from figures 10-11 that CAD for maximum rate of pressure rise is concentrated near the average value of CAD maximum rate of pressure rise $\theta_{(dP/d\theta)_{max}}$. It can be observed from the figures 10-11 that average $\theta_{(dP/d\theta)_{max}}$ is before TDC for all test points at intake air temperatures 120^{0}C for gasoline. It can also be observed that maximum repeatability of $\theta_{(dP/d\theta)_{max}}$ is up to 60% for all engine operating conditions using methanol and gasoline fuels. It can also be observed from the figures that, for both fuels (methanol and gasoline) repeatability of CAD maximum rate of pressure rise increases as mixture becomes leaner for constant intake air temperature.

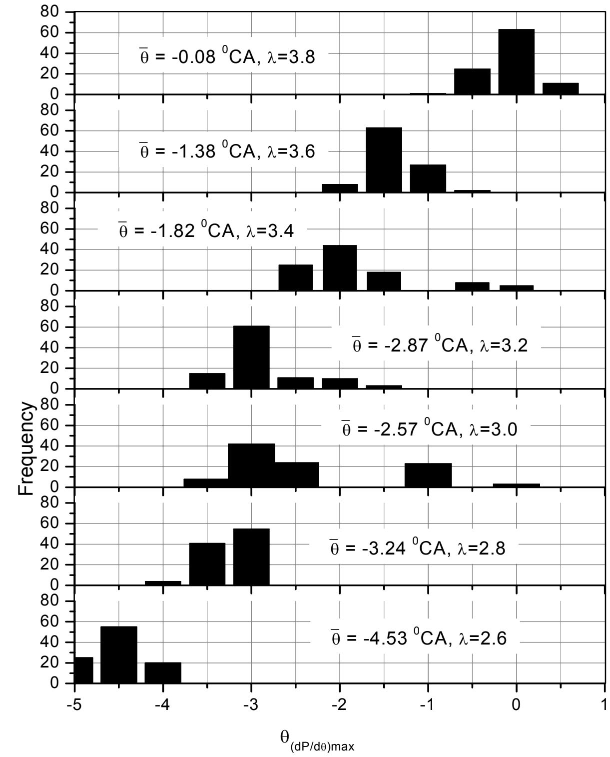

Figure 11: Frequency distribution of crank angle corresponding to $(dP/d\theta)_{max}$ at intake air temperature 120 ^{0}C for gasoline

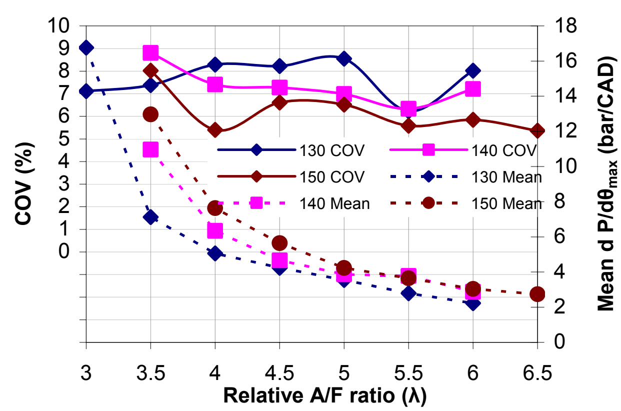

Figure 12: Cycle-to-cycle variation of $(dP/d\theta)_{max}$ for methanol

Figures 12-13 show the cycle-to-cycle variations of rate of pressure rise using methanol and gasoline at different intake air temperatures and air fuel mixtures. These figures also show COV and mean maximum rate of pressure rise for 100 cycles at each test conditions for both fuels. Similar trends are observed at all intake air temperatures for both fuels in terms of COV and average maximum rate of pressure rise. Average $(dP/d\theta)_{max}$ decreases as mixture becomes leaner at any constant intake air temperature.

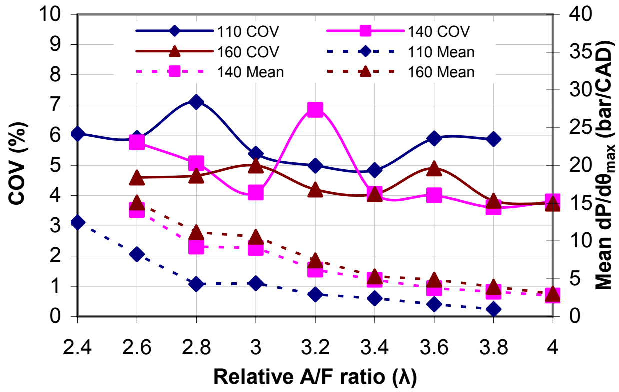

Figure 13: Cycle-to-cycle variation of $\left(dP/d\theta\right)_{max}$ for gasoline

For any air-fuel ratio, average rate of pressure rise increases with increase in intake air temperature of the engine. It can also be observed from these figures that with increasing intake air temperature, the COV decreases. Maximum rate of pressure deviate to large range as compared to maximum pressure inside the combustion chamber during combustion. It can be noticed from figures 12-13 that COV of $\left(dP/d\theta\right)_{max}$ is lower for gasoline as compared to methanol. The value of COV of rate of pressure rise for gasoline is up to 7% for all the test conditions but in case of methanol up to 13% for given engine operating conditions.

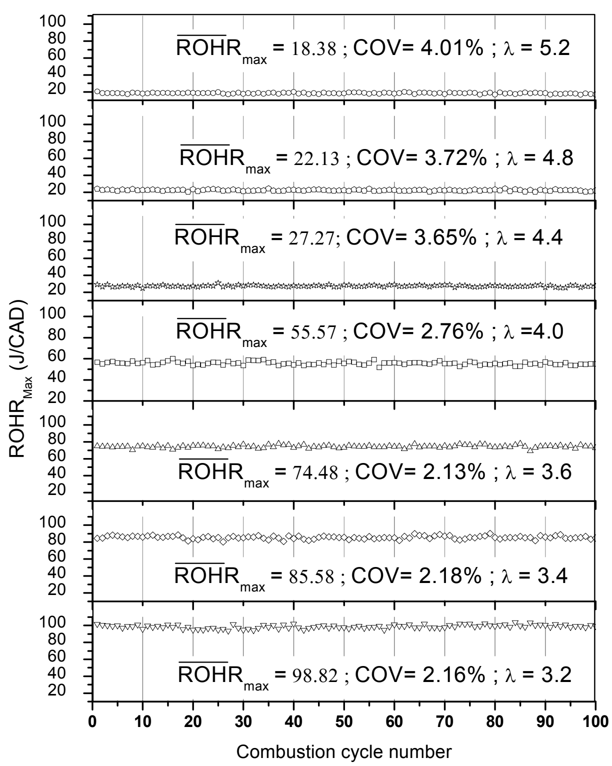

Figure 14: Cycle-to-cycle variation of $ROHR_{max}$ at intake air temperature 120^{0}C for methanol

Figures 14-17 show the cycle-to-cycle variation of peak value of ROHR and corresponding crank angle for maximum ROHR at all engine test conditions for both fuels. ROHR is measure of how fast chemical energy of fuel is converted to the thermal energy by combustion. This directly affects rate of pressure rise and accordingly the power produced. It is necessary that cycle-to-cycle variation of ROHR is within specified limit for smooth engine operation.

For all plots (Figure 14), average value of $ROHR_{max}$ was highest corresponding for engine operation with richest mixture, and the lowest corresponding to leanest mixture at any given intake air temperature. Due to advanced ignition timing of the rich fuel/ air mixture, the peak values of the heat release rate are very high for richer fuel-air mixture. Figures 14-15 show that COV of $ROHR_{max}$ is lower for richer fuel-air mixtures. It can also be noticed that cycle-to-cycle variation of $ROHR_{max}$ is less than 5 percent for all operating conditions for gasoline as well as methanol at 120^{0}C intake air temperature. This indicates that cycle-to-cycle variation of rate of heat release is low at these experimental conditions..

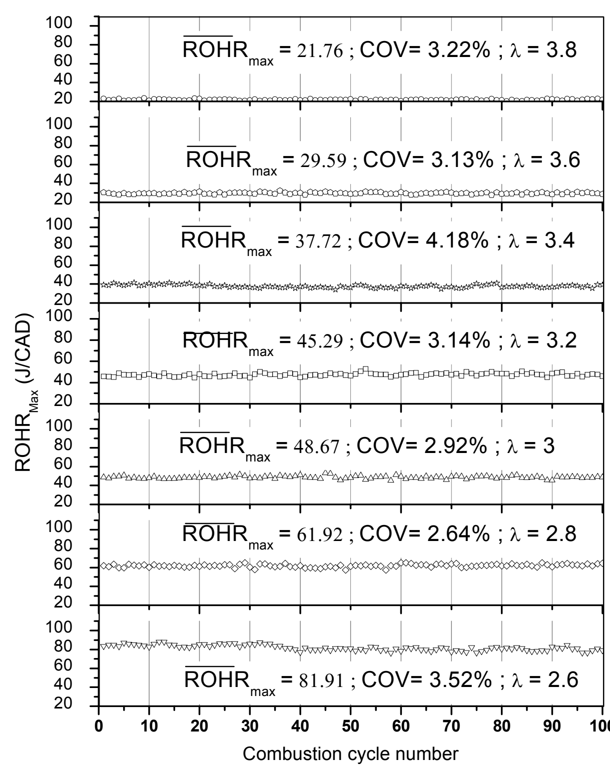

Figure 15: Cycle-to-cycle variation of $ROHR_{max}$ at intake air temperature 120^{0}C for gasoline

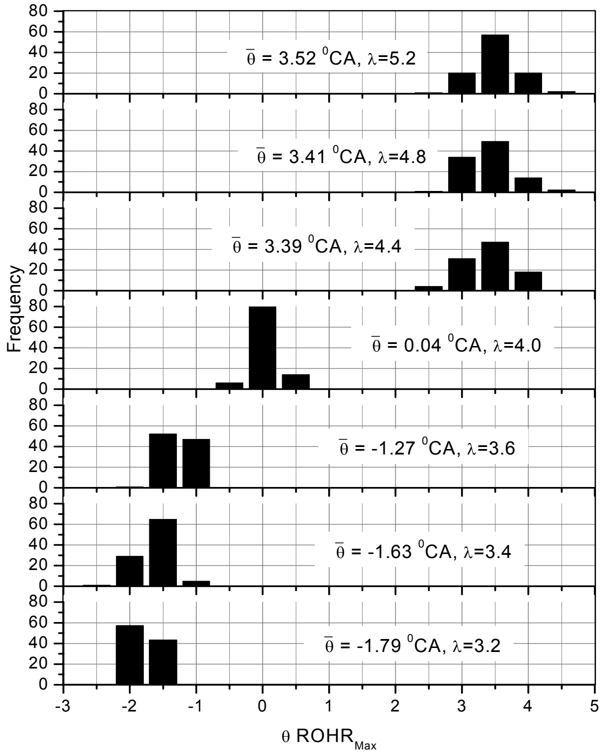

Figure 16: Frequency distribution of crank angle corresponding to $ROHR_{max}$ at intake air temperature 120^0C for methanol

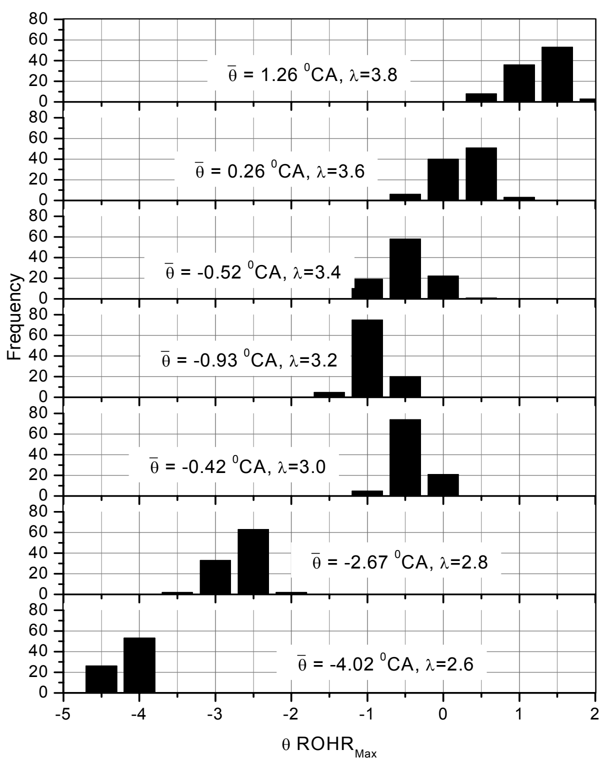

Figure 17: Frequency distribution of crank angle corresponding to $ROHR_{max}$ at intake air temperature 120^0C for gasoline

Figures 16-17 show frequency distribution of CAD of $ROHR_{max}$. It can be observed from these figures that average value of CAD for $ROHR_{max}$ is very close to TDC.

It can be noticed from figures 16-17 that average value of CAD $ROHR_{max}$ is moving away from TDC as engine was operates on leaner mixture at a constant intake air temperature for both gasoline and methanol. Figures also show that the crank angle location of $ROHR_{max}$ is concentrated in a very close range to the peak value of CAD $ROHR_{max}$ and its spread is very limited. It is observed that repeatability of same CAD of maximum ROHR is up to 75% for gasoline and up to 80% in methanol. It can also be noticed that for both methanol and gasoline, repeatability of CAD $ROHR_{max}$ increases as mixture becomes leaner for constant intake air temperature.

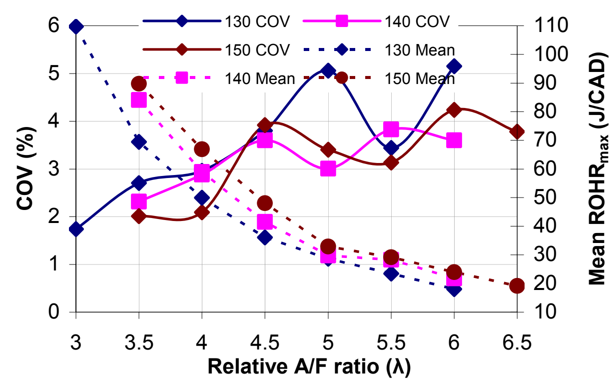

Figure 18: Cycle-to-cycle variation of $ROHR_{max}$ for methanol

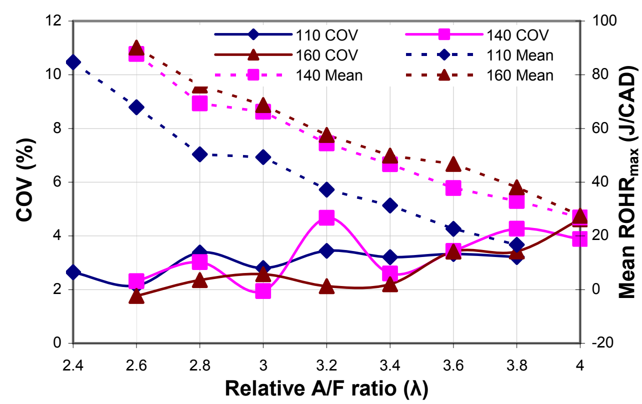

Figure 19: Cycle-to-cycle variation of $ROHR_{max}$ for gasoline

Figures 18-19 shows the cycle-to-cycle variation of $ROHR_{max}$ using methanol and gasoline at different intake air temperatures and air-fuel ratios. These figures show COV and average maximum rate of heat release for 100 cycles at each test conditions for both fuels. Mean values are represented by dotted lines and COV are connect by solid lines. Identical trend is observed for all intake air temperatures for both fuels in terms of COV and average rate of heat release. Average $ROHR_{max}$ decreases as mixture becomes leaner at any constant intake air temperature. It can also be noticed from the figures that average value of $ROHR_{max}$ increases with increase in intake air temperature for any given air-fuel ratio. It can also be noticed from figures 18 and19 that COV of $ROHR_{max}$ is lower for both fuel and it is less than 5 percent for all engine operating conditions.

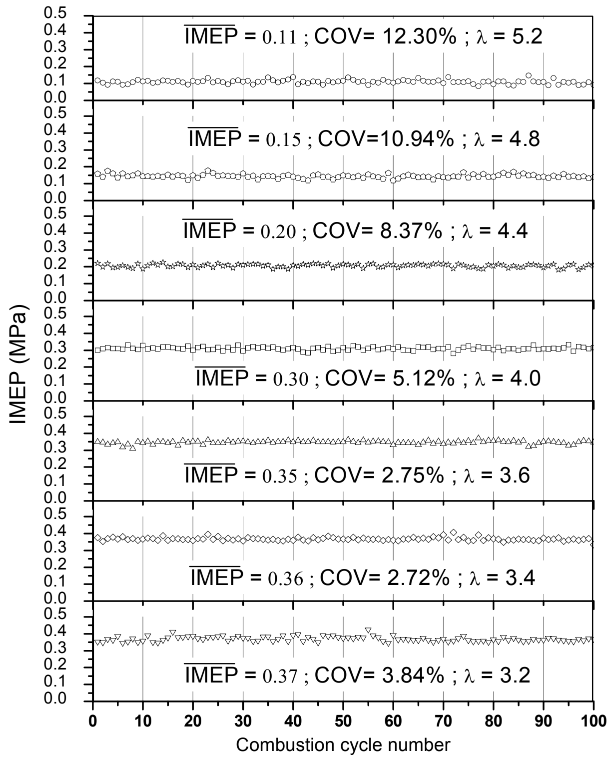

Figure 20: Cycle-to-cycle variation of IMEP at intake air temperature 120^{0}C for methanol

It is important to investigate the cycle-to-cycle variation of IMEP because it directly affects the engine drivability. It is reported [22] that drivability problems in automobiles normally arise when COV of IMEP exceeds 10 percent, hence this parameter can be used for investigation of the lower boundary condition for HCCI combustion. One major limitation of HCCI combustion is the requirement of a highly diluted fuel-air mixture in order to slow down the speed of the chemical reactions sufficiently so that engine is not damaged by extremely high ROHR and this leads to rather slower combustion. With lean operation, this will significantly reduce the output for a given air flow through the engine. The rich side limit for IMEP is limited by the rate of combustion and hence rate of pressure rise.

Figures 20-21 illustrate the cycle-to-cycle variations of IMEP at all test point for 100 consecutive combustion cycles at intake air temperature of 120^{0}C. It is observed that the average value of IMEP is decreasing as engine operates on leaner mixtures. This trend is similar for both methanol and gasoline. It can be noticed from figures 20-21 that COV of IMEP increases with increase in λ (i.e. leaner mixture). The COV is lowest for richest fuel-air mixture at any intake air temperature for both fuels. For leaner engine operating conditions, COV of IMEP can be greater than 10 percent. This is observed for the both fuels at leanest mixtures..

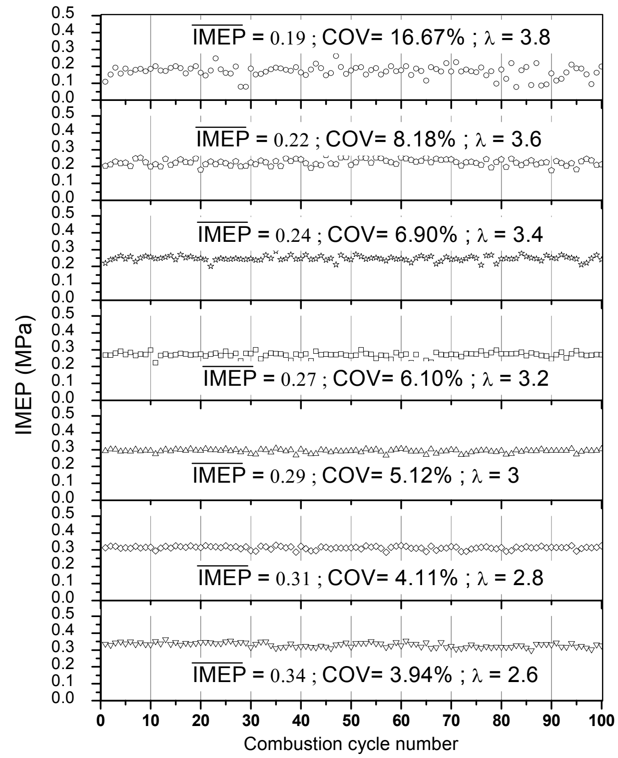

Figure 21: Cycle-to-cycle variation of IMEP at intake air temperature 120^{0}C for gasoline

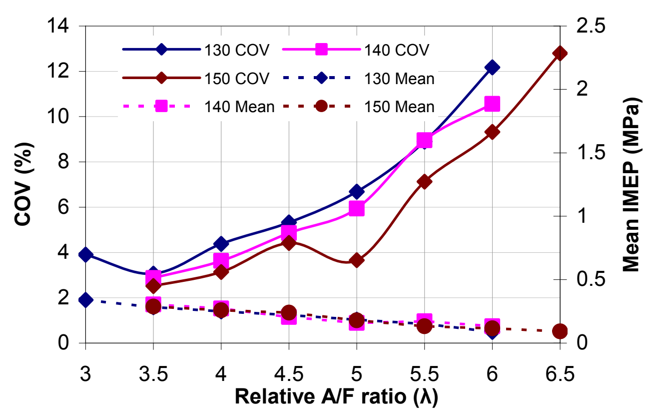

Figure 22: Cycle-to-cycle variation of IMEP for methanol

Figures 22-23 show cycle-to-cycle variations of IMEP using methanol and gasoline at different intake air temperatures and air-fuel mixtures. Figures show COV and average IMEP for 100 consecutive cycles at each test conditions for both fuels. Similar trends are observed at all intake air temperatures for both fuels in terms of COV and average IMEP. Average value of IMEP decreases as mixture becomes leaner at any constant intake air temperature. At any air-fuel ratio, the COV decrease with increase in intake air temperature. These figures show that COV of IMEP exceeds 10% for some test conditions. Hence the COV of IMEP should be used as a criterion for lower boundary condition for HCCI operating range.

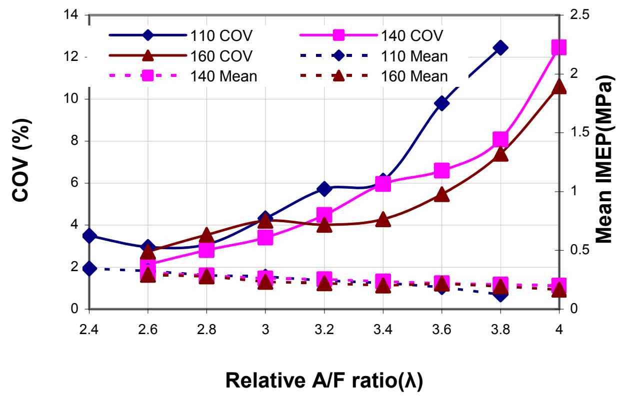

Figure 23: Cycle-to-cycle variation of IMEP for gasoline

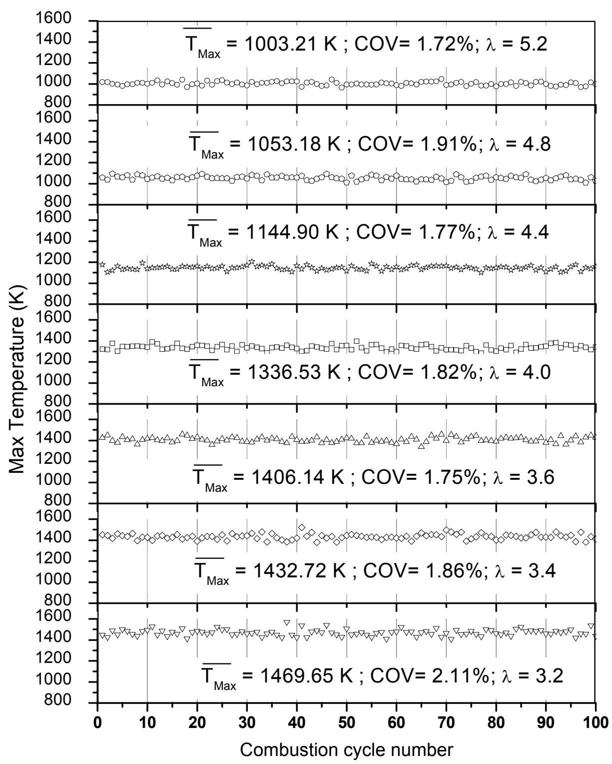

Figure 24: Cycle-to-cycle variation of T_{max} at intake air temperature 120^{0}C for methanol

It is worth examining the cycle-to-cycle variation of maximum average gas temperature inside the cylinder since it is directly related to emissions from the engine for HCCI combustion. With homogeneous combustion of a premixed charge, the temperature is expected to be same throughout the combustion chamber, except near the walls. This, in combination with very lean fuel-air mixtures gives low maximum temperature during the cycle. NOx formation is very sensitive to peak temperature encountered during the combustion. At temperatures above 1800 K, NOx formation rate increases rapidly. Large variations in mean gas temperature give rise to variation of NOx emissions as well. Figures 24-27 show the cycle-to-cycle variation of the maximum gas temperature of 100 consecutive combustion cycles for methanol and gasoline fuels.

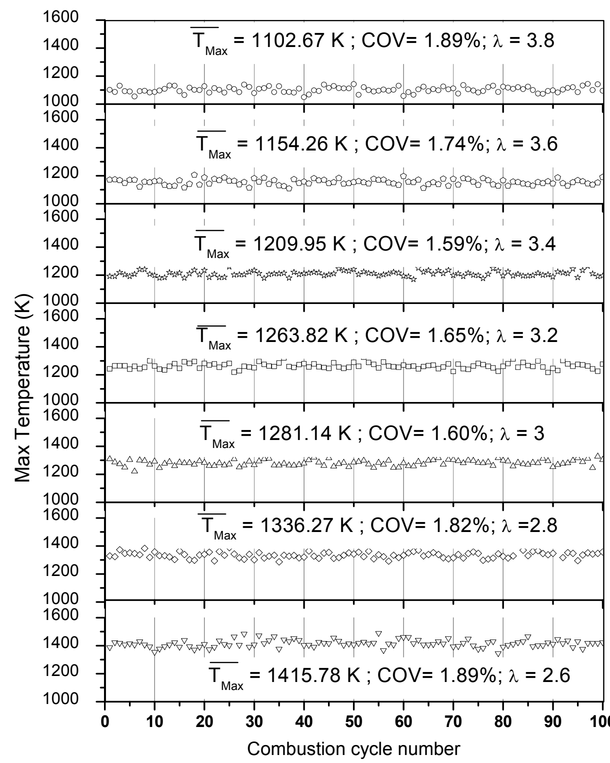

Figure 25: Cycle-to-cycle variation of T_{max} at intake air temperature 120^{0}C for gasoline

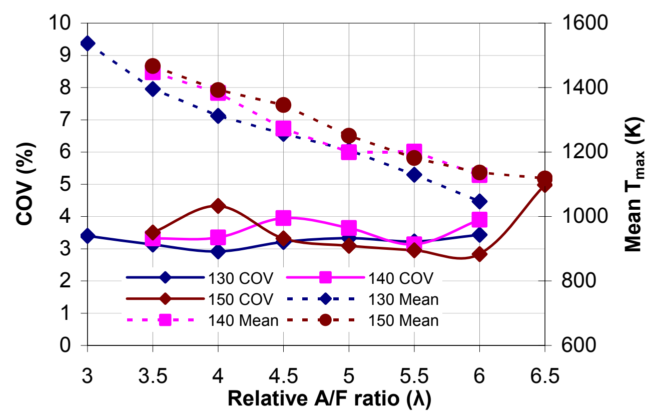

Figure 26: Cycle-to-cycle variation of T_{max} for methanol

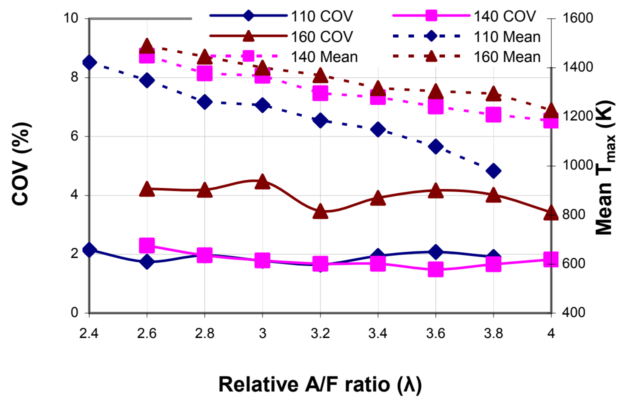

Figure 27: Cycle-to-cycle variation of T_{max} for gasoline

It can be noticed that the average value of T_{max} decreases with increasing value of λ (i.e. leaner mixtures) at any given intake air temperature. Average T_{max} in combustion cycles increases with increase in intake air temperature. It can be noticed that COV of T_{max} was smaller for both methanol and gasoline for intake air temperature of 120^{0}C.

Figures 26-27 show the cycle-to-cycle variation of T_{max} using methanol and gasoline at different intake air temperature and air fuel mixtures. These figures also show COV and average T_{max} of 100 consecutive cycles at each test conditions for both fuels. It can be noticed that identical trends are observed at all intake air temperatures for both fuels in terms of COV and average T_{max}. Average value of T_{max} decreases as mixture becomes leaner at any constant intake air temperature. The value of COV at all engine operating conditions is smaller for both fuels and it is less than 5%, hence that the statistical variation is rather small in HCCI combustion.

Table 1: COV of different parameters for methanol HCCI combustion

	λ	P_{max}	dP/dθ	IMEP	$ROHR_{Max}$	T_{max}
120^{o}C	3.2	1.91	7.22	3.84	2.16	2.11
	3.4	1.29	7.34	2.72	2.18	1.86
	3.6	0.92	6.98	2.75	2.13	1.75
	4	0.87	7.73	5.12	2.76	1.82
	4.4	0.85	12.06	8.37	3.65	1.77
	4.8	0.76	12.47	10.94	3.72	1.91
	5.2	0.69	13.31	12.3	4.01	1.72
130^{o}C	3	1.955	7.112	3.908	1.741	3.401
	3.5	1.037	7.38	3.055	2.705	3.132
	4	0.737	8.29	4.376	2.96	2.916
	4.5	0.729	8.225	5.329	3.801	3.212
	5	0.768	8.55	6.684	5.059	3.33
	5.5	0.558	6.226	8.903	3.441	3.225
	6	0.692	8.021	12.176	5.154	3.434
140^{o}C	3.5	1.199	8.805	2.868	2.316	3.321
	4	0.802	7.403	3.632	2.88	3.348
	4.5	0.634	7.269	4.861	3.6	3.952
	5	0.597	6.979	5.938	3.01	3.641
	5.5	0.759	6.33	8.956	3.827	3.136
	6	0.797	7.205	10.563	3.602	3.9
150^{o}C	3.5	1.292	8.023	2.515	2.012	3.505
	4	0.776	5.4	3.136	2.09	4.328
	4.5	0.792	6.611	4.421	3.917	3.321
	5	0.523	6.515	3.66	3.402	3.093
	5.5	0.537	5.584	7.13	3.134	2.952
	6	0.661	5.843	9.324	4.236	2.835
	6.5	0.479	5.362	12.798	3.78	4.977

Table 2: COV of different parameters for gasoline HCCI combustion

	λ	P_{max}	dP/dθ	IMEP	$ROHR_{Max}$	T_{max}
110^{o}C	2.4	1.294	6.046	3.493	2.648	2.151
	2.6	0.763	5.908	2.965	2.155	1.748
	2.8	0.675	7.097	3.087	3.376	1.966
	3	0.503	5.387	4.319	2.8	1.781
	3.2	0.627	4.988	5.727	3.444	1.649
	3.4	0.638	4.84	6.119	3.206	1.94
	3.6	0.739	5.893	9.801	3.323	2.079
	3.8	0.811	5.872	12.453	3.211	1.91
120^{o}C	2.6	1.32	6.25	3.94	3.52	1.89
	2.8	0.68	5.47	4.11	2.64	1.82
	3	0.5	5.41	5.12	2.92	1.6
	3.2	0.52	6.16	6.1	3.14	1.65
	3.4	0.58	4.93	6.9	4.18	1.59
	3.6	0.59	4.51	8.18	3.13	1.74
	3.8	0.88	5.57	16.67	3.22	1.89
140^{o}C	2.6	0.786	5.76	2.128	2.315	2.294
	2.8	0.74	5.061	2.813	3.018	1.965
	3	0.74	4.104	3.408	1.943	1.789
	3.2	0.529	6.839	4.483	4.672	1.679
	3.4	0.382	4.053	5.96	2.6	1.677
	3.6	0.424	4.004	6.601	3.442	1.484
	3.8	0.416	3.611	8.081	4.268	1.658
	4	0.418	3.803	12.466	3.881	1.823
160^{o}C	2.6	0.801	4.597	2.744	1.765	4.227
	2.8	0.692	4.663	3.537	2.353	4.193
	3	0.621	4.993	4.208	2.572	4.478
	3.2	0.588	4.202	4.016	2.13	3.466
	3.4	0.339	4.051	4.281	2.2	3.916
	3.6	0.393	4.899	5.477	3.413	4.175
	3.8	0.398	3.831	7.41	3.421	4.019
	4	0.416	3.739	10.616	4.618	3.421

The values of COV of different combustion parameters for methanol and gasoline are presented in tables 1-2 for all engine operating conditions. It can be observed that there are two critical parameters, (i) rate of pressure rise and (ii) IMEP for which value of COV exceeds 10%. Variation in these two parameters is important for smooth engine operation in HCCI combustion mode.

CONCLUSIONS

The cycle-to-cycle variations in combustion and performance parameters of HCCI combustion were investigated in a HCCI engine. The engine was operated at a constant engine speed of 1500 rpm with port fuel injection of methanol and gasoline in HCCI mode. It was found that at lower intake air temperature, it is possible to ignite the richer mixture (up to $\lambda = 2.4$ for gasoline and $\lambda = 3$ for methanol) in HCCI mode. As intake air temperature increase, engine running on richer mixture makes engine operation noisier. But at higher intake air temperature it is possible to ignite the leaner mixture in HCCI combustion mode.

COV of P_{max} increases with increasingly richer mixture and COV increases with increase in intake air temperature. For all test points, the variation in maximum in-cylinder pressure is small (COV< 2%) and repeatability of CAD of P_{max} is less than 60% for methanol and up to 70% for gasoline. For both methanol and gasoline, repeatability of CAD P_{max} increases as mixture becomes leaner for constant intake air temperature.

Average value of rate of pressure rise ($dP/d\theta$) is an important parameter for HCCI operating range criteria compared to COV of maximum pressure rise rate. Cycle-to-cycle variation of maximum rate of pressure is lower for gasoline as compared to methanol at intake air temperature of 120^0C. The variation in the maximum pressure rise rate is more than 10% for some of the test conditions. Maximum repeatability of $\theta_{(dP/d\theta)_{max}}$ is up to 65% for all engine operating conditions using methanol and gasoline fuels**.**

Cycle-to-cycle variation of $ROHR_{max}$ is less than 5% for all operating conditions for gasoline and methanol. It is observed that repeatability of same CAD of maximum ROHR is up to 75% for gasoline and up to 80% for methanol.

The COV of IMEP increases with the increase of λ (leaner mixture) and decreases with the increase in intake air temperature. The COV of IMEP exceeds 10% for some of the test conditions. It is a critical parameter for the HCCI combustion engine. Hence the critical parameters that can be used to define the HCCI operating range are the maximum pressure rise rate and COV of IMEP.

REFERENCES

1. Onishi, S., Jo, S.H., Shoda, K., Jo, D.P., Kato, S., Active Thermo-Atmosphere Combustion (ATAC) – A New Combustion Process for Internal Combustion Engines, SAE Paper 790501, 1979.
2. Noguchi, M., Tanaka, T., Takeuchi Y., A Study On gasoline Engine Combustion by Observation of Intermediate Reactive Products during Combustion, SAE Paper 790840, 1979.
3. Zhoa, F., Asmus, T.W., Assanis, D.N., Dec, J.E., Eng, J.A., Najt, P.M., Homogeneous Charge Compression Ignition (HCCI) Engines Key Research and Development Issues, SAE Warrendale, PA, ISBN 0-7680-1123-X, 2003.
4. Ishibashi, Y., Asai M., Improving the Exhaust Emissions of Two-Stroke Engines by Applying the Activated Radical Combustion, SAE Paper 960742, 1996.
5. Najt, P.M., Foster, D.E., Compression-Ignited Homogeneous Charge Combustion, SAE Paper 830264, 1983.
6. Thring, R.H., Homogeneous-Charge Compression-Ignition (HCCI) Engine, SAE Paper 892068, 1989.
7. Aoyama, T., Hattori, Y., Mizuta J., Sato, Y., An Experimental Study on Premixed-Charge Compression Ignition Gasoline Engine, SAE Paper 960081, 1996
8. Yanagihara, H.A., A Simultaneous Reduction of NOx and Soot in Diesel Engines under a New Combustion System (uniform bulky combustion system UNIBUS), 17th. Int. Motor Symposium, Vienna, 1996.
9. Yokota, H., Kudo, Y., Nakajima, H., Kakegawa, T., Susuki, T., A New Concept for Low Emission Diesel Combustion, SAE Paper 970891, 1997.
10. Christensen, M., Johansson, B., Einewall, P., Homogeneous Charge Compression Ignition (HCCI) Using Isooctane, Ethanol and Natural Gas – A Comparison with Spark-Ignition Operation, SAE Paper 972874, 1997.
11. Christensen, M., Johansson, B., Amnjus, P., Mauss, F., Supercharged Homogeneous Charge Compression Ignition, SAE Paper 980787, 1998.
12. Stanglmaier, R.H., Rayan III, T.W., Souder J.S., HCCI Operation of a Dual-Fuel Natural Gas Engine for Improved Fuel Efficiency and Ultra Low NOx Emissions at Low to Moderate Engine Loads, SAE Paper 2001-01-1897, 2001.
13. Walter, B., Gatellier B. (2003). Near Zero NOx Emissions and High Fuel Efficiency Diesel Engine: the NADI™ Concept Using Dual Mode Combustion. Oil & Gas Science and Technology Rev. IFP, 58 (1).
14. Puschmann, H., Buchwald, R., Pannwitz A., Sommer, A., Homogeneous Diesel Combustion with External Mixture Formation by Cool Flame Vaporizer, SAE Paper 2006-01-3323, 2006.

15. Takeda, Y., Keiichi, N., Emission Characteristics of Premixed Lean Diesel Combustion with Extremely Early Staged Fuel Injection, SAE Paper 961163, 1996.
16. Iwabuchi, Y., Kawai, K., Shoji, T., Takeda, Y., Trial of New Concept Diesel Combustion System-Premixed Compression-Ignited Combustion, SAE Paper 1999-01-0185, 1999.
17. Kimura, S., Aoki, O., Ogawa, H., Muranaka, S., Enomoto, Y., New Combustion Concept for Ultra-Clean and High-Efficiency Small DI Diesel Engines, SAE Paper 1999-01-3681, 1999.
18. Kelly-Zion, Peter, L., John, D. E., A computational Study of the effect of the Fuel-Type on the Ignition Time in HCCI Engines, Proceedings of Combustion Institute. 28, 2000.
19. Xingcai, L., Libin, J., Junjun, M., Zhen, H. (2007). Experimental Study on the Cycle-by-Cycle Variations of Homogeneous Charge Compression Ignition Combustion Using Primary Reference Fuels and Their Mixtures. Proc. Instn Mech. Engrs, Part D: J. Automobile Engineering, 221(7).
20. Iida, M., Hayashi, M., Foster, D. E., Martin, J. K. (2003). Characteristics Of Homogeneous Charge Compression Ignition (HCCI) Engine Operation for Variations in Compression Ratio, Speed, and Intake Temperature While Using N-Butane as A Fuel, Journal of Engineering for Gas Turbines and Power, 125 (2).
21. Iida, M., Aroonsrisopon, T., Hayashi, M., Foster, D. Martin, J., The Effect of Intake Air Temperature, Compression Ratio and Coolant Temperature on the Start of Heat Release in an HCCI (Homogeneous Charge Compression Ignition) Engine, SAE paper 2001-01-1880, 2001.
22. Heywood, J.B., Internal Combustion engine fundamentals, McGraw-Hill Book Company, NewYork, 1988.
23. Yong, M.B., Cyclic Dispersion in the Homogeneous Charge Spark-Ignition Engine - A Literature Survey, SAE Paper 810020, 1981.
24. Soltau, J.P., Cylinder Pressure Variations in Petrol Engine, Proceedings of the institution of mechanical engineers, Vol.2, 1960-1961.
25. Stone, C. R., Brown, A. G., Beckwith P., Cycle-by-Cycle Variations in Spark Ignition Engine and Combustion – Part II: Modeling of Flame Kernel Heat Release Analysis on Combustion and Displacements as A Cause of Cycle-by-Cycle Variations, SAE paper 960613, 1996.
26. Ball, J. K., Raine, R. R., Stone, C. R. (1998). Combustion Analysis and Cycle-by-Cycle Variations in Spark Ignition Engine Combustion – Part 1: An Evaluation of Combustion Analysis Routines by Reference to Model Data. Proc. Instn Mech. Engrs, Part D: J. Automobile Engineering, 212(5).
27. Ball, J. K., Raine, R. R., Stone, C. R. (1998). Combustion Analysis and Cycle-by-Cycle Variations in Spark Ignition Engine Combustion – Part 2: A New Parameter for Completeness of Combustion and its Use in Modeling Cycle-by-Cycle Variations in Combustion. Proc. Instn Mech. Engrs, Part D: J. Automobile Engineering, 212(6).
28. Huang, Z., Shiga, S., Ueda, T., Nakamura, H., Ishima, T., Obokata, T., Tsue, M., Kono, M. (2003). Study of Cycle-by-Cycle Variations of Natural Gas Direct Injection Combustion using A Rapid Compression Machine, Proc. Instn Mech. Engrs, Part D: J. Automobile Engineering, 217(1).
29. Persson, H., Pfeiffer, R., Hultqvist, A., Johansson, B., Stro¨m, H., Cylinder-to-Cylinder and Cycle-to Cycle Variations at HCCI Operation with Trapped Residuals, SAE paper 2005-01-0130, 2005.
30. Koopmans, L., Backlund, O., Denbratt, I., Cycle to Cycle Variations: Their Influence on Cycle Resolved Gas Temperature and Unburned Hydrocarbons from a Camless Gasoline Compression Ignition Engine, SAE paper 2002-01-0110, 2002.
31. Shi, L., Deng, K. Cui, Y. (2007). Combustion Stability of Diesel-Fueled HCCI. International Journal of Automotive Technology, 8 (4).
32. REVelation Operator Reference Manual, Hi-Techniques, Inc. Madison, USA, 2004, pp. 95-96.

CONTACT

Rakesh Kumar Maurya is a Graduate student working with Dr. Agarwal on his doctoral dissertation in mechanical engineering from IIT Kanpur. He completed his Dual Degree (B.Tech. and M.Tech.) from IIT Kanpur in Mechanical Engineering in year 2006. His areas of interest include Internal Combustion Engines, Engine Instrumentation, HCCI Combustion, and emission control.

Dr. Avinash Kumar Agarwal is currently working as Associate Professor of Mechanical Engineering at Indian Institute of Technology, Kanpur. He is a 1994 Mechanical Engineering graduate from MREC Jaipur. His area of doctoral research was developing biodiesel and related engine tribology investigations. Dr Agarwal joined Engine Research Center, University of Wisconsin, Madison, USA for pursuing his Post-Doctoral research from August 1999 – February 2001. His main areas of current interest are combustion phenomenon study in IC engines, automobile emissions, biodiesel development and characterization, laser diagnostic techniques, PIV, lubricating oil consumption phenomenon, lubricating oil tribology, development of micro sensors, alternative fuels for diesel engines etc.